Influence of higher-order stimulated Brillouin scattering on the occurrence of extreme events in self-pulsing fiber lasers

Djamila Boukhaoui,[1] Djouher Mallek,[1] Abdelhamid Kellou,[1] Hervé Leblond,[2] François Sanchez,[2] Thomas Godin,[3,*] and Ammar Hideur[3,†]

[1]*Laboratoire d'Electronique Quantique, Université des Sciences et de la Technologie H. Boumediene, Algiers, Algeria*

[2]*Laboratoire de Photonique d'Angers EA4464, Université d'Angers, Angers, France*

[3]*CORIA UMR6614, Normandie Université, CNRS-INSA-Université de Rouen Normandie, Normandy, France*

(Received 16 May 2019; published 8 July 2019)

We investigate the dynamical behavior of a self-pulsing laser under the influence of stimulated Brillouin scattering (SBS), a system which has previously been shown to favor extreme statistics. Using a laser model coupling a multi-Stokes Brillouin scattering process with the population inversion formalism for the gain and taking into account saturable absorption effects, we demonstrate that different statistical distribution types arise as the nonlinear interactions between the laser and higher-order SBS waves lead to the occurrence of high intensity short pulses. By taking into account up to five Stokes orders, we show that highly skewed statistics and pulses with extreme peak intensities can be obtained, allowing us to describe more accurately the experimental observations and to better apprehend the underlying physics. We also unexpectedly demonstrate that the acoustic noise does not affect the emergence of such extreme events.

DOI: 10.1103/PhysRevA.100.013809

I. INTRODUCTION

Extreme instabilities in optics have aroused constant interest for more than a decade in a myriad of varied systems [1–3]. Specifically in dissipative systems, such as Raman fiber lasers, laser diodes, or mode-locked lasers, to name a few, long-tailed statistics and highly localized temporal structures have been observed [4–8]. Recent studies showed that stimulated Brillouin scattering (SBS) can also trigger the generation of extreme events in various configurations, from self-pulsing fiber lasers [9] to Q-switched random fiber lasers [10] and high-power fiber amplifiers [11]. It is indeed known that the stochastic nature of SBS can promote the emergence of randomly distributed giant pulses which can induce irreversible damage in fiber laser systems.

In order to understand and open the possibility to harness such extreme events, numerical models have then to be developed and refined. In the context of rare-earth-doped fiber lasers and amplifiers, several studies taking into account one fundamental Stokes order or a cascade of several Stokes components have already been reported [12–14]. Taking into account the random nature of SBS, these coupled waves models reproduce the temporal pulse structures observed experimentally in fiber lasers and amplifiers under the influence of SBS [12,13,15]. They also describe relatively well the large pulse-to-pulse intensity fluctuations observed in SBS-based Q-switched erbium-doped fiber lasers but, however, do not predict the occurrence of any extreme event [13]. It has only recently been demonstrated that the extension of this coupled waves model by including the effect of laser reabsorption by rare-earth ions inside a high-loss cavity can provide more insights on the temporal dynamics of such highly dissipative systems [9]. Such a model is based on the coupled amplitudes equations describing the spatiotemporal dynamics of both the laser and a single Stokes wave with its corresponding acoustic field, as well as the temporal variations of the gain for each wave. It also considers a matter equation to account for the saturable absorption effect which can occur in the unpumped segment of the active fiber. The numerical simulations show that for a large set of parameters the model predicts the emergence of temporally localized structures with high intensities exhibiting all the features of rogue events with highly skewed intensity distributions [9]. However, the peak power predicted for this structure remains much lower than that observed in the experiments [9], where it has even been shown that these high-intensity pulses can reach the damage threshold of passive fibers [10,12]. There is thus a need for improving the accuracy of this model to precisely reproduce the experimental features and to fully understand the underlying physics. It has also been shown numerically, albeit in a different frame, that cascaded Brillouin laser operating at high powers can exhibit very rich dynamics and strong intensity fluctuations as new noise channels are opened by cascaded lasing [16]. In this paper, we thereby present an extension of our previous model taking into account multiple higher-order Stokes waves within the resonator and investigate their influence on the occurrence of extreme events.

The paper is structured as follows. We first investigate the impact of high-order Stokes waves on the dynamics of a self-Q-switched ytterbium doped-fiber laser. We study how increasing the number of SBS orders interacting with the gain medium reveals new dynamics by enabling the generation of extreme events with giant amplitudes which are not predicted

*thomas.godin@coria.fr
†hideur@coria.fr

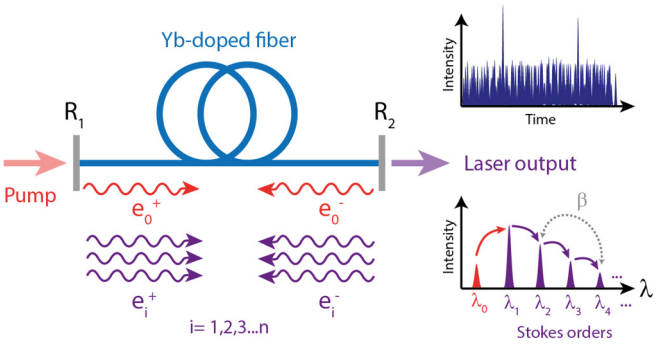

FIG. 1. Schematic representation of the cascaded Brillouin fiber Fabry-Pérot resonator with multiple forward and backward generated Stokes waves, denoted e_i^+ and e_i^-, respectively. Forward and backward laser waves are denoted e_0^+ and e_0^-, respectively. β represents the coupling between Stokes orders.

by a single SBS order model but also influences the pulse duration. In the second part, the influence of the stochastic response of spontaneous Brillouin scattering is investigated by adding a Langevin noise source term in the equations governing the evolution of the acoustic waves [13]. By disabling the saturable absorber effect, the numerical calculations predict a chaotic pulsed operation with a probability density function (PDF) following an exponential law, thus indicating that the stochastic processes are not the origin of the extreme events generation. We finally discuss the different research directions opened by this work.

II. INFLUENCE OF CASCADED SBS ON SELF-PULSING DYNAMICS

Here, we consider the simplified Fabry-Pérot fiber laser cavity schematically depicted in Fig. 1 and comprising an ytterbium-doped fiber and two plane mirrors with reflectivities R_1 and R_2. In this cavity, forward and backward propagating waves are considered for laser as well as for Stokes waves with different orders. In the following, the model we propose is solved numerically using a fourth-order Runge-Kutta algorithm for the time domain and a finite difference algorithm for the spatial domain.

A. General model of high-orders stimulated Brillouin scattering

The influence of stimulated Brillouin scattering with one fundamental Stokes order on the laser dynamics in high-loss linear cavities can be accounted for using a coupled amplitude model [9,17]. The latter is based on a rate-equations model including transitions such as stimulated and spontaneous emissions as well as stimulated Brillouin scattering and allows the description of phenomena occurring on a time scale well above the phonon lifetime. We consider here an inhomogeneously broadened gain in the laser medium which is included in a Fabry-Pérot cavity. If the generation of Stokes waves up to the nth order is taken into account, the model then involves $n+2$ matter equations and their $(2n+2)$ field equations, the forward and backward laser components, Stokes waves, and $2n$ field equations for acoustic waves. Regarding saturation effects, only the cross saturation between nearest neighbors can be taken into account to describe the laser dynamics [18]. Assuming linear polarization for light waves and slowly varying envelopes for all the waves while neglecting the influences of optical Kerr effect and Raman scattering then yields the following dimensionless model:

$$\frac{\partial d_i}{\partial T} = \gamma_i\, p - a_1(d_i+1) - 2d_i[|e_i^+|^2 + |e_i^-|^2 + \beta(|e_{i-1}^+|^2 + |e_{i-1}^-|^2 + |e_{i+1}^+|^2 + |e_{i+1}^-|^2)], \quad (1)$$

$$\frac{\partial d_{as}}{\partial T} = -a_{as}(d_{as}+b_1) - 2d_{as}\Sigma\left(\sum_{i=0}^{n}(|e_i^+|^2 + |e_i^-|^2)\right), \quad (2)$$

$$\left(\frac{\partial}{\partial T} \pm \frac{\partial}{\partial Z}\right)e_i^\pm = g_c(e_{ai}^{\mp *}e_{i-1}^\mp - e_{ai+1}^\pm e_{i+1}^\mp) + \left(\frac{1}{2}A_{as}d_{as} - \frac{\alpha_c}{2}\right)e_i^\pm + \frac{A_c}{2}[d_i + \beta(d_{i-1}+d_{i+1})]e_i^\pm, \quad (3)$$

$$\frac{\partial e_{aj}^\pm}{\partial T} = \alpha_a(e_{j-1}^\pm e_j^{\mp *} - ea_j{}^\pm) + f_j{}^\pm(Z,T). \quad (4)$$

In this model, we consider by convention that e_{-1}, d_{-1}, e_{n+1}, and d_{n+1} are null. The d_i $(i=0,\ldots,n)$ are the population inversions normalized with the concentration D_0 of active ions and associated to the laser and Stokes waves, d_{as} is the population inversion normalized with the concentration of effective saturable absorber, and $e_{i=0,\ldots,n}^\pm$ are the normalized amplitudes of the laser and Stokes orders. $e_{aj}^\pm$ $(j=1,\ldots,n)$ correspond to the acoustic fields amplitudes. The superscript plus and minus stand for the forward and backward components, respectively. The different fields are coupled through the cross-saturation parameter β [19,20] and a matter equation is considered to account for the saturable absorption effect [21,22], which can occur in the unpumped segment of the active fiber [23]. The time $T = t/T_r$ is normalized with the photon travel time along the fiber (T_r) and the longitudinal coordinate $Z = z/L$ is normalized with the fiber length (L), which is assumed to coincide with the total cavity length, so that the normalized cavity length is $l = 1$. $f_j{}^\pm(Z,T)$ is the Langevin noise source describing spontaneous Brillouin scattering and consisting in a Gaussian stochastic process with zero mean [13,24].

Taking into account appropriate boundary conditions at the input and output $(z = l)$ mirrors (with reflection coefficients $R_1 > 99\%$ and $R_2 = 4\%$) yields the following equations:

$$e_i^+(0,T) = \sqrt{R_1}e_i^-(0,T), \quad (5)$$

$$e_i^-(l,T) = \sqrt{R_2}e_i^+(l,T), \quad (6)$$

$$\Sigma = \frac{\sigma_{as}}{\sigma}, \quad a_1 = a_{as} = \frac{T_r}{\tau}, \quad A_c = A_{as} = \tau d_0 L,$$

$$g_c = \frac{g_B L I_0}{2}, \quad \alpha_c = \alpha L, \quad \alpha_a = \frac{T_r\Gamma}{2}, \quad I_0 = \frac{\hbar\omega}{\sigma T_r}.$$

TABLE I. Parameters used in the numerical simulations of the laser self-pulsing behavior with cascaded Brillouin orders.

D_0	10^{24} m^{-3}	Active ions concentration
T_r	48 ns	Photon travel time
L	10 m	Fiber length
τ	800 μs	Popul. inversion lifetime
g_B	1.66×10^{-11} m W^{-1}	Brillouin gain
g_c	100	Norm. Bril. gain
α	0.0458 m^{-1}	Abs. coefficient
σ	32×10^{-25} m^2	Em. cross section
σ_{as}	32×10^{-25} m^2	Sat. abs. cross section
$\gamma_{0\to5}$	1, 0.7, 0.55, 0.35, 0.25, 0.15	Dichroism
β	0.5	Cross saturation
b_1	0.5	Saturable absorber parameter
Γ	625×10^5 s^{-1}	Acoustic wave damping coef.
p	(0.367 to 1.1)$\times 10^{-3}$ m^{-3}/s	Pumping param.
$r = p/p_{th}$	4 to 12	Pump/threshold

The different parameters in these equations and their numerical values used in our simulations are listed in Table I. ω is the optical pulsation and γ_i represent the dichroism in the pumping for each population inversion and for each Stokes order. β is the cross-saturation parameter and physically represents the strength of the coupling between the laser and the Stokes fields [the $(i-1)$th Stokes the i^{th} and $(i+1)$th Stokes orders] through the amplifying medium. The laser threshold is then written as follows:

$$p_{th} = \frac{a_1}{(1+\beta\gamma_1)}\left[1+\beta+\frac{1}{A_c}\left(\alpha_c + A_{as}b_1 + \frac{1}{2l}\ln\frac{1}{R_1R_2}\right)\right]. \tag{7}$$

Earlier experimental observations show that increasing the pump power above the laser threshold yields to the emergence of several Stokes components from such linear cavity configuration [9,25,26]. In the following section, we choose to limit the study to five interacting Stokes orders as it already yields remarkable insights into the understanding of extreme events generation while keeping the computation time reasonable.

B. Numerical results and discussion

1. Model with saturable absorption

In our previous work taking into account only a single Stokes order [9], the numerical model predicted self-pulsing operation with microsecond pulses near threshold, while nanosecond transients with high-peak powers are obtained at higher pumping levels. For the conception of this model, the self-pulsing behavior is mainly attributed to the reabsorption of the laser photons within the fiber [25–27]. The single-ended pumping of the fiber associated with the quasi-three-level transition scheme of ytterbium can then result in a high absorption section for low pumping levels, acting as an effective saturable absorber [23]. For the sake of clarity, we recall typical results in this configuration in Figs. 2(a) and 2(b), where high-intensity nanosecond events are observed along with a highly skewed distribution of the intensities, as shown in Fig. 3(a) with more than 200 extreme events captured over a total of 2.1×10^6 events. Although allowing to roughly represent the extreme dynamics observed experimentally, this model is quite limited, as for higher pumping rates the experimental observations are not reproduced anymore. Indeed, events with peak amplitudes of more than five times the rogue wave intensity threshold (twice the significant wave height parameter) have been observed experimentally, while the numerically predicted peak amplitudes are less than twice the rogue wave threshold [9]. Moreover, experiments show that these high-intensity pulses can reach the multi-kW level and subsequently induce irreversible damages in fiber laser systems [10,12].

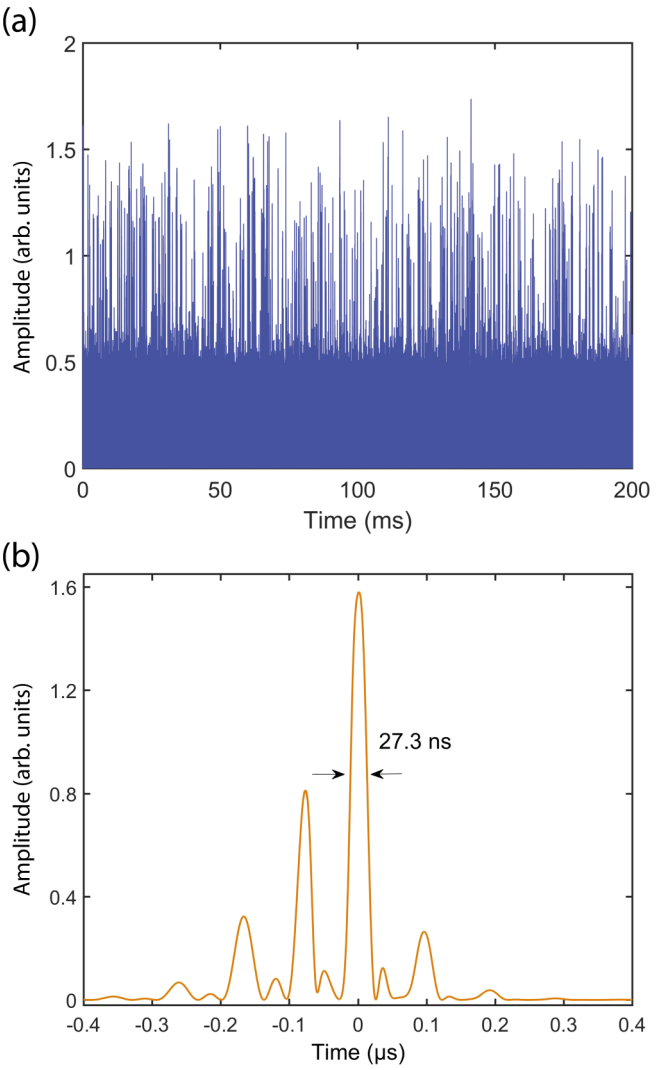

FIG. 2. (a) Time trace obtained after the numerical resolution of the single SBS order model ($r = 8$). (b) Detail of typical intense pulses.

In order to better match these experimental observations, we then now implement an extended model involving cascaded Stokes orders in the SBS process, coupled to a

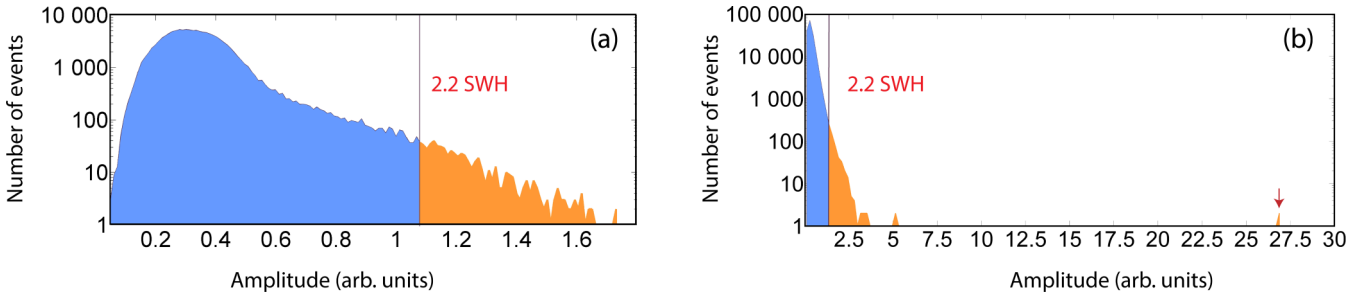

FIG. 3. Pulse amplitude distributions in the self-pulsing laser when considering (a) a single Stokes order and (b) five Stokes orders. The vertical dotted lines represent the extreme event limit, using the standard SWH criterion.

population inversion model of the inhomogeneous gain. We first neglect the influence of Langevin noise (stochastic noise source) and take up to five Stokes orders into account. For a pumping ratio $r = 8$ (i.e., eight times the laser threshold), the temporal dynamics and corresponding statistical distribution then also exhibit an extreme behavior, as highlighted in the time traces in Fig. 4 and by the amplitude distribution in Fig. 3(b), with a consequent amount of events randomly distributed in time and exceeding twice the significant wave height (SWH), which qualify them as "rogue." We also notice the emergence of a giant pulse with an amplitude higher than 25 times the SWH as shown in Fig. 4(a) and with a closeup in Fig. 4(b). It is worth noting that these results are numerically reproduced for different temporal and spatial resolutions and at different pump levels. In this case nearly 800 events over 3×10^6 are considered as extreme. Further increasing the pump level to $r = 12$ allows for the generation of extreme events with even higher amplitudes, as shown in Fig. 5. It is worth highlighting that such a behavior was not reproducible using the single Brillouin order model. In experiments, such optical intensities would then cause irreversible damage to the optical fibers, and this behavior has precisely been reported in such cavities [28].

In order to quantitatively compare the single and high-order models and their impact on the system dynamics, return intensity maps can be relevant indicators. Such a map plots the intensity of the $(k + n)$th event as a function of the intensity of the (k)th, where extreme events are revealed by points moving away from the average due to their high amplitudes. Return intensity maps comparing both models for different pumping levels are then presented in Fig. 6. We here choose $n = 10$ to highlight the particular dynamics observed in these simulations. It can clearly be seen from the map in Fig. 6(b) that taking into account five Stokes orders instead of one leads to a largely increased instability, which is closer to actual observations.

In both cases, however, no extreme events are reported when lowering the pumping level to $r = 4$, i.e., below the Brillouin threshold, as seen in Fig. 6(a). Nevertheless, for $r = 8$, the return intensity map in Fig. 6(b) exhibits a specific behavior with two arms with increased lengths and higher dispersion which can now be considered as signatures of extreme dynamics. The higher dispersion between consecutive events can be understood as the emergence of a giant pulse with maximum amplitude which benefits from a substantial accumulated gain in the amplifying medium compared to the previous events. Moreover, the difference in amplitude between consecutive events in the generation process can be observed in the amplitude distributions in Fig. 3(b), where there is a large gap in amplitude between the pulse with maximum amplitude (∼27) and the closest one (∼5). Our

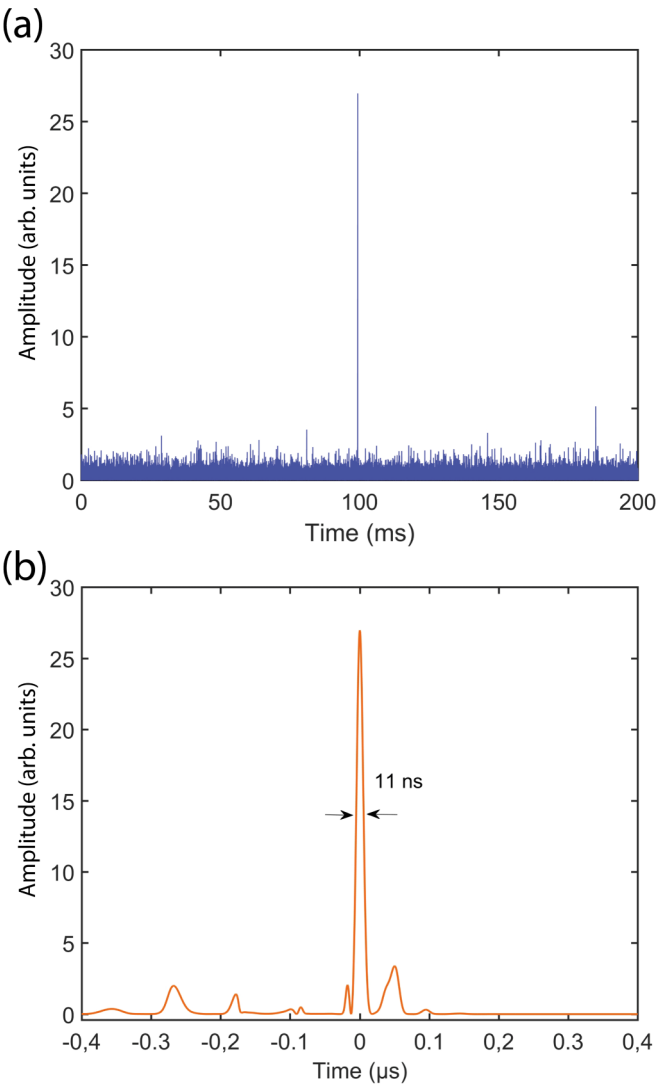

FIG. 4. (a) Time trace obtained after the numerical resolution of our model in 200 ms for five Stokes orders ($r = 8$). (b) Details of the extreme pulse substructure.

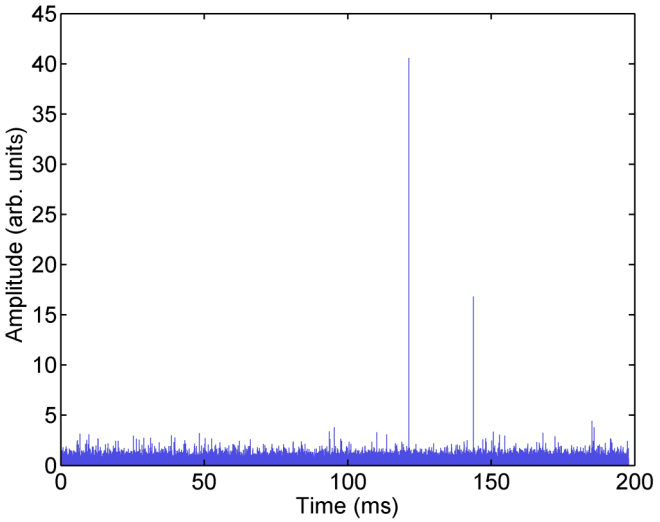

FIG. 5. Temporal sequences of output pulses considering five Stokes orders in the cavity with $r = 12$.

findings also show that increasing the number of Stokes orders leads to pulse shortening as shown on Fig. 7, in which the number of Stokes orders is varied from one to five. The corresponding pulse duration is then decreased from 27.3 ns for a single SBS order to 12 ns for five orders, that we can attribute to an increased stochasticity of the system. It is worth noting that the pulse structures are different in both cases: for a single Stokes order considered only, the pulse exhibits several nanosecond substructures with average amplitudes, as shown in Fig. 2(b), whereas, when considering higher Stokes orders, the pulse is mainly composed by a single nanosecond structure with extreme amplitude, as shown in Fig. 4(b).

As a conclusion for this section, taking into account higher-order cascaded Brillouin scattering in the self-pulsing dynamics dramatically increases the system stochasticity, thus leading to extreme events peak-power scaling and pulse duration shortening, then giving birth to so-called "fast" extreme events according to the recent classification by Klein and co-workers [29]. Our findings are consistent with experimental observations in slightly different conditions, e.g., in Refs. [10,11,30]. It is worth mentioning that such behaviors have only been observed in laser cavities comprising heavily ytterbium-doped gain fibers which are very auspicious for self-pulsing laser operation, which in turn serves as a pump for SBS generation at relatively low threshold. In order to bring more consistency to our approach, we investigate in the next section the influence of acoustic noise on the system dynamics independent of the saturable absorption effect.

2. *Other parameters influencing laser dynamics and perspectives for further refinements*

When dealing with SBS, it is commonly assumed that two sources mainly drive the acoustic waves generation [24]: (i) the thermal fluctuations in the fiber considered as acoustic noise and giving rise to spontaneous Brillouin scattering and (ii) the electrostriction effect in the presence of a laser field, initiating stimulated Brillouin scattering. In this section, we discuss the influence of such an acoustic noise on the

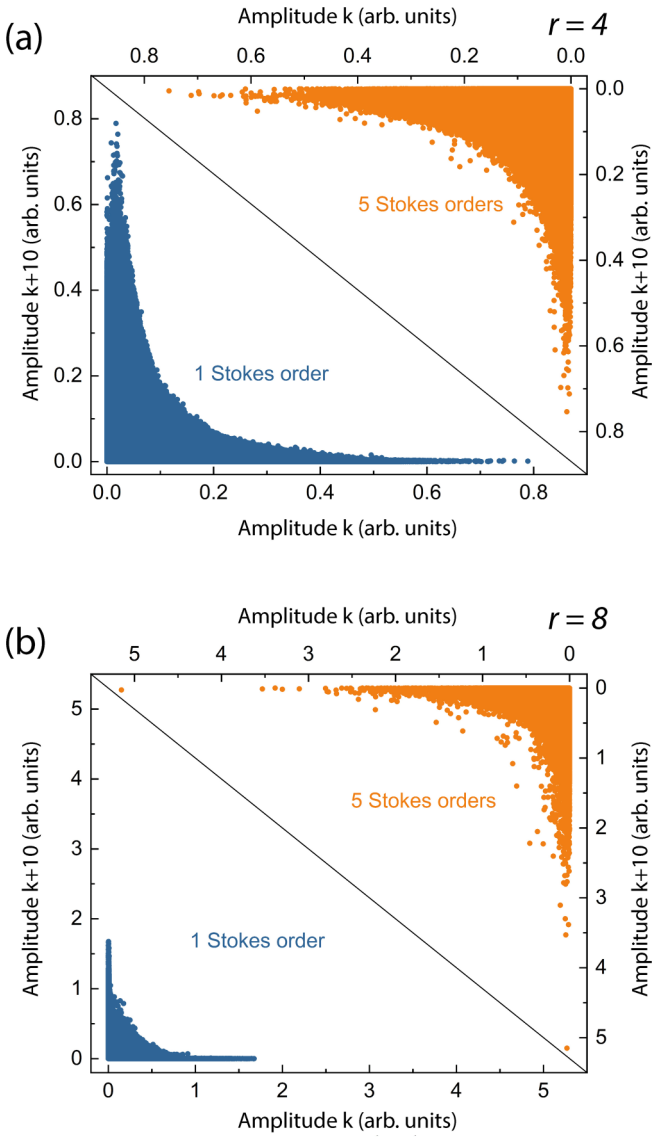

FIG. 6. 10th return intensity maps in configurations taking into account the first Stokes order only (blue) or five Stokes orders (orange) for (a) a pumping ratio $r = 4$, i.e., below the Brillouin threshold, and for (b) $r = 8$, i.e., above the Brillouin threshold. *NB*: in the $r = 8$ case with five Stokes orders, extreme amplitudes are not displayed for better clarity. Data are recorded on 200 ms time sequences.

self-pulsing laser dynamics while neglecting the saturable absorption effect previously considered. A Langevin noise term $f_j^{\pm}(Z, T)$ is thereby added in the equations governing the acoustic waves evolution and the strength of this term can be derived from thermodynamic considerations. This Langevin noise source is δ correlated in space and time and is a Gaussian random process with zero mean [12,24,31]:

$$\langle f_j^{\pm}(Z, T) \cdot f_j^{\pm}(Z', T') \rangle = Q\delta(T - T') \cdot \delta(Z - Z'), \quad (8)$$

with Q being the dimensionless strength of the acoustic noise, defined as

$$Q = \frac{k_B T \Gamma_B^2 v_g T_r}{2 g_B I_0^2 L A v_s}, \quad (9)$$

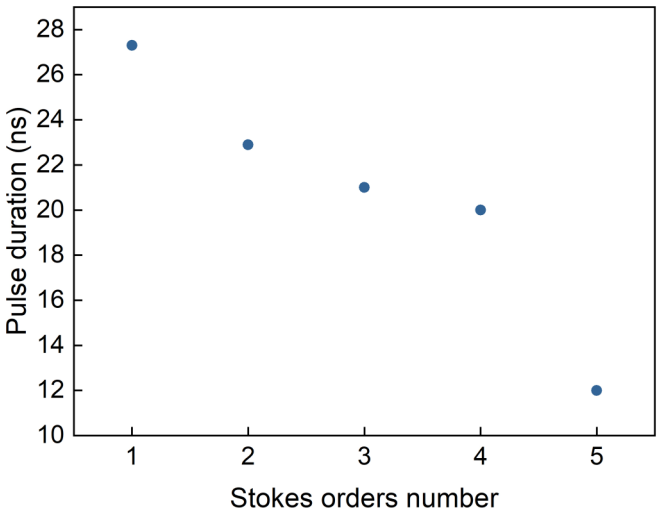

FIG. 7. Evolution of pulse duration as a function of the number of Stokes orders considered in the numerical model, for a fixed pumping level and equivalent amplitudes.

where k_B is the Boltzmann constant, T is the temperature, and v_g and v_s are the laser wave group velocity and acoustic wave velocity, respectively. A is the mode field area. This noise source is implemented using a standard random numbers generator and then converted to a Gaussian random number using a Box-Muller transform. In this case, numerical calculations still predict self-pulsing regimes with chaotic dynamics but without any events considered as extreme. As already shown by Fotiadi *et al.* [13], the Langevin noise source gives rise to chaotic behaviors with intensity distribution following an exponential law, thus minimizing its role in the emergence of the extreme event.

It is also worth noting that the choice of the pump dichroism parameters is not critical in the observation of extreme events in our laser system and similar behaviors have indeed been obtained for other sets of γ_i parameters.

As a perspective for this study, a next step would be to take higher Stokes orders into account, as multiple orders up to a few tens have already been reported experimentally [26]. The model could also take into account other linear and nonlinear processes to fully match with experiments, such as Rayleigh and Raman scatterings. For Rayleigh scattering, it is here assumed that its impact is quite limited due to the short segments of fiber considered. It has also been shown experimentally that the peak powers of the short pulses generated through cascaded SBS could reach the Raman threshold intensity, thus leading to intracavity Raman supercontinuum generation [32]. However, the associated laser dynamics has never been investigated under such conditions and work is now in progress regarding this point.

III. CONCLUSION

In this paper, we numerically investigated the influence of cascaded stimulated Brillouin scattering on the extreme dynamics of a self-pulsing heavily ytterbium-doped fiber laser. We then developed a spatiotemporal model which couples multi-Stokes Brillouin scattering and population inversion mechanisms. This model also takes into account the saturable absorption effects resulting from signal absorption in the unpumped part of the gain fiber and a Langevin noise source. Our findings show that taking into account higher Stokes orders in the SBS process has a remarkable impact on the laser dynamics as it enables the generation of giant pulses which cannot be observed with a single Stokes order model. These different behaviors have been highlighted by typical amplitude distributions and return maps in both cases. Even if we limited the study to five Stokes orders, our model reproduces more accurately the experimental observation of rogue events in such laser systems. In addition, we have shown that the higher the number of Stokes orders considered, the shorter are the extreme pulses. Our study also reveals that SBS noise has a negligible role in the emergence of the extreme events which are mainly driven by the effective saturable absorber mechanism. This work then paves the way for building a complete general model involving other linear and nonlinear processes such as SRS and Kerr effects, which will be a valuable tool for the investigation of the underlying nonlinear dynamics in dissipative laser systems.

ACKNOWLEDGMENTS

This work was supported by the French Agence Nationale de la Recherche (LabEx EMC3 program and RIFT Project No. ANR-15-CE08-0018-01), the European Union with the European Regional Development Fund, and the Regional Council of Normandie. D.B. acknowledges support from the French-Algerian PROFAS B+ program.

[1] J. M. Dudley, F. Dias, M. Erkintalo, and G. Genty, Nat. Photon. **8**, 755 (2014).

[2] N. Akhmediev, B. Kibler, F. Baronio, M. Belić, W. Zhong, Y. Zhang, W. Chang, J. Soto-Crespo, P. Vouzas, P. Grelu, C. Lecaplain, K. Hammani, S. Rica, A. Picozzi, M. Tlidi, K. Panajotov, A. Mussot, A. Bendahmane, P. Szriftgiser, G. Genty, J. Dudley, A. Kudlinski, A. Demircan, M. U., S. Amiraranashvili, C. Bree, G. Steinmeyer, C. Masoller, N. Broderick, A. Runge, M. Erkintalo, S. Residori, U. Bortolozzo, F. Arecchi, S. Wabnitz, C. Tiofack, S. Coulibaly, and M. Taki, J. Opt. **18**, 063001 (2016).

[3] M. Sciamanna and K. A. Shore, Nat. Photon. **9**, 151 (2015).

[4] A. F. Runge, C. Aguergaray, N. G. Broderick, and M. Erkintalo, Opt. Lett. **39**, 319 (2014).

[5] S. Perrone, R. Vilaseca, J. Zamora-Munt, and C. Masoller, Phys. Rev. A **89**, 033804 (2014).

[6] C. Lecaplain, P. Grelu, J. M. Soto-Crespo, and N. Akhmediev, Phys. Rev. Lett. **108**, 233901 (2012).

[7] S. D. Chowdhury, B. D. Gupta, S. Chatterjee, R. Sen, and M. Pal, Opt. Lett. **44**, 2161 (2019).

[8] A. E. Akosman and M. Y. Sander, Sci. Rep. **8**, 13385 (2018).

[9] P. H. Hanzard, M. Talbi, D. Mallek, A. Kellou, H. Leblond, F. Sanchez, T. Godin, and A. Hideur, Sci. Rep. **7**, 45868 (2017).
[10] A. V. Kir'yanov, Y. O. Barmenkov, and M. V. Andres, Laser Phys. Lett. **10**, 055112 (2013).
[11] Y. Panbhiharwala, A. V. Harish, D. Venkitesh, J. Nilsson, and B. Srinivasan, Opt. Express **26**, 33409 (2018).
[12] G. Kulcsar, Y. Jaouen, G. Canat, E. Olmedo, and G. Debarge, IEEE Photon. Technol. Lett. **15**, 801 (2003).
[13] A. A. Fotiadi, P. Mégret, and M. Blondel, Opt. Lett. **29**, 1078 (2004).
[14] M. Laroche, H. Gilles, and S. Girard, Opt. Commun. **281**, 2243 (2008).
[15] M. Laroche, H. Gilles, and S. Girard, Opt. Lett. **36**, 241 (2011).
[16] R. O. Behunin, N. T. Otterstrom, P. T. Rakich, S. Gundavarapu, and D. J. Blumenthal, Phys. Rev. A **98**, 023832 (2018).
[17] D. Mallek, A. Kellou, H. Leblond, and F. Sanchez, Opt. Commun. **308**, 130 (2013).
[18] C. Szwaj, S. Bielawski, and D. Derozier, Phys. Rev. Lett. **77**, 4540 (1996).
[19] F. Sanchez, M. LeFlohic, G. M. Stephan, P. LeBoudec, and P.-L. Francois, IEEE J. Quantum Electron. **31**, 481 (1995).
[20] F. Sanchez and G. Stephan, Phys. Rev. E **53**, 2110 (1996).
[21] L. Luo and P. L. Chu, Opt. Commun. **161**, 257 (1999).
[22] S. D. Jackson, Electron. Lett. **38**, 1640 (2002).
[23] D. Marcuse, IEEE J. Quantum Electron. **29**, 2390 (1993).
[24] A. L. Gaeta and R. W. Boyd, Phys. Rev. A **44**, 3205 (1991).
[25] A. Hideur, T. Chartier, C. Özkul, and F. Sanchez, Opt. Commun **186**, 311 (2000).
[26] M. Salhi, A. Hideur, T. Chartier, M. Brunel, G. Martel, C. Ozkul, and F. Sanchez, Opt. Lett. **27**, 1294 (2002).
[27] W. P. Risk, J. Opt. Soc. Am. B **14**, 3457 (1997).
[28] B. Ortaç, A. Hideur, T. Chartier, M. Brunel, G. Martel, M. Salhi, and F. Sanchez, Opt. Commun. **215**, 389 (2003).
[29] A. Klein, G. Masri, H. Duadi, K. Sulimany, O. Lib, H. Steinberg, S. A. Kolpakov, and M. Fridman, Optica **5**, 774 (2018).
[30] Y. Tang and J. Xu, Sci. Rep. **5**, 9338 (2015).
[31] A. A. Fotiadi and R. V. Kiyan, Opt. Lett. **23**, 1805 (1998).
[32] S. V. Chernikov, Y. Zhu, J. R. Taylor, and V. P. Gapontsev, Opt. Lett. **22**, 298 (1997).